

WORCESTER POLYTECHNIC INSTITUTE
MAJOR QUALIFYING PROJECT REPORT

WIRELESS WEARABLE CORE BODY TEMPERATURE SENSOR

May 6, 2021

This report represents the work of one or more WPI undergraduate students submitted to the faculty as evidence of completion of a degree requirement. WPI routinely publishes these reports on the web without editorial or peer review.

ADVISOR

Professor Ulkuhan Guler
uguler@wpi.edu

UNDERGRADUATE STUDENTS

Eric Baccei
Electrical and Computer Engineering
ecbaccei@wpi.edu

Eric Macorri
Electrical and Computer Engineering
emacorri@wpi.edu

Cameron Williams
Electrical and Computer Engineering
cbwilliams@wpi.edu

Contents

Abstract	3
Executive Summary	4
List of Figures	6
List of Tables	7
1. Introduction	8
1.1. Motivations	8
1.1.1. Heat Related Illnesses	9
1.1.2. CBT Monitoring	11
1.2. Current State of the Art	12
1.2.1. Zero-Heat Flux	12
1.2.2. Dual-Heat Flux	13
2. Project Overview	15
2.1. Design	15
2.2. Project Organization	15
2.3. Project Challenges	16
3. Background Research	17
3.1. Sensor Design	17
3.1.1. Sensor Size and Insulation	18
3.1.2. Heat Transducers	19
3.2. Electrical Design	20
3.2.1. Multiplexer	20
3.2.2. Signal Amplification	20
3.2.3. Filtering	20
3.2.4. Microcontrollers	21
4. Proposed Design and Implementation	22
4.1. Proposed Sensor Design	22
4.2. Proposed Analog Front End Design	23
4.2.1. PCB Design	24
4.3. Microcontroller, Wireless Protocol, and Mobile App	25
4.3.1. Microcontroller Options	25

5. Hardware Test Implementation	27
5.1. Sensor	27
5.2. Transducers	28
5.2.1. Thermistor	28
5.2.2. Analog Sensors	29
5.3. Operational Amplifier	30
5.4. Active Filter	30
5.5. Breadboard and Printed Circuit Board	30
5.6. Microcontroller	32
5.6.1. Code and Implementation	32
6. System Integration and Data Analysis	33
6.1. Human Test Implementation	33
6.2. Water Bath Testing	34
7. Recommendations	37
7.1. Transducer Considerations	37
7.1.1. Sensor Accuracy vs Rate of Change	37
7.1.2. Sensor Size	37
7.2. Physical Design Considerations	38
7.2.1. Cover Material and Design	38
7.2.2. Insulating Material	38
7.3. Microcontroller and Mobile App	38
7.3.1. Data Acquisition	39
7.3.2. Power Reduction	39
7.3.3. User Interface	39
8. Conclusion	40
Acknowledgment	41
Appendix A. Decision Matrices	44
Appendix B. Microcontroller Firmware	45
B.1. Data Acquisition using ADC	45
B.2. Convert Data from mV to °C	45
B.3. Transmit Data to Smartphone via BLE	45

Abstract

Core body temperature (CBT) falls under the list of vitals that must be closely monitored in many settings, such as a patient going through surgery or a soldier in the battlefield. Although the importance is major, there are not many devices that can do this remotely and non-invasively. Our project designed a wearable device that can noninvasively monitor CBT based on the Dual-Heat Flux Method (DHFM). The device is able to communicate wirelessly with a personal computer through Bluetooth Low Energy (BLE). This wireless and low power device is able to monitor the CBT of a person whether they are moving, sitting, or lying down over long periods of time.

Executive Summary

The human body must maintain a specific core body temperature (CBT) in order to sustain itself and operate properly. A typical CBT lies around 37°C (98.6°F), but can range between 36.5°C (97.7°F) and 37.5°C (99.5°F). If a person's CBT were to drop too low or rise too high, they run the risk of hypothermia or hyperthermia, which could potentially be fatal. Temperatures can vary depending on a lot of factors, such as environment, activity, age, time of day, etc. This makes continuous and accurate measurement of CBT very important.

There are multiple ways to measure CBT. Most of the gold standard measurements involve invasive methods such as intubation during surgery or thermometry through aural, oral, or rectal means. Although these methods have their importance and proper uses, all of them are invasive and many do not have continuous monitoring capability. These methods are very limited in cases where an individual would need continuous, noninvasive, and wireless monitoring such as during exercise. Therefore, research has been conducted to find noninvasive and continuous monitoring. Two promising methods include Zero Heat Flux (ZHF) and Dual-Heat Flux (DHF). Zero heat flux works by having temperature transducers between a heating element that would be placed on the body. The heating element would bring the sensor to equilibrium so that the heat transducers could measure the CBT of the body accurately. DHF follows a similar principle without the use of a heating element, which would drastically reduce power consumption. This method uses four temperature transducers placed within a main insulator that would be placed on the body in order to extract the CBT.

The focus of this Major Qualifying Project (MQP) is to develop and design a wireless, noninvasive, and continuous CBT sensor. To achieve this goal, we build a sensor utilizing DHF, send the output signal through an Analog Front End (AFE) for amplification and filtering, and process the signal through a micro-controller in order to send the data over bluetooth. We choose DHF because we didn't need a heating element which in turn would reduce our overall power consumption and make battery operation more plausible. Once the heat extraction method was chosen, we began our design process with block diagram of our device shown in Figure 1.

Since there are four heat transducers within the sensor, we chose a multiplexer in order to pass through one of the signals at a time. The micro-controller would control the signal flow of the multiplexer. Once the signal had been chosen by the multiplexer, it would pass through a non-inverting operational amplifier and then be filtered. The AFE was then built on a breadboard to be tested and once it had passed using predetermined signals, a PCB build had been initiated. Concurrently with PCB

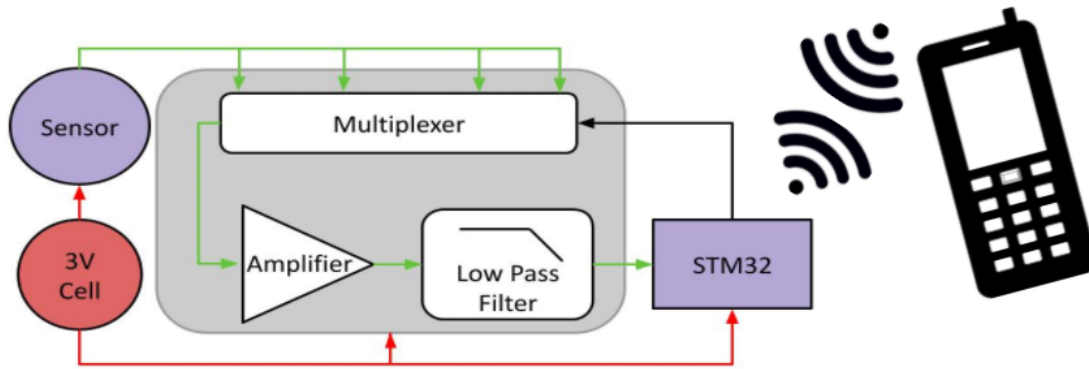


Figure 1: High-level system overview.

development, the sensor construction had began. We decided to design the sensor using Computer Aided Design (CAD) and 3D print a cover to hold the insulation and heat transducers. The next step was to configure the micro-controller ADC, IO, and logic in order to receive, process, and output the data through bluetooth. Once all designs had been completed, we ran a test to verify each block and their interactions with each other.

Due to the affects of COVID-19 during this project's process, we were unable to conduct testing on human subjects besides ourselves. We also conducted experiments utilizing a water bath to set and measure specific temperatures. After verification of all the electrical components had been completed, we ran a human test by affixing the sensor to our forehead and extracting data. Although the device operated properly, we were unable to achieve significant results. We were within 3°C error of the expected value during our human trials. After the human test, we attached the sensor to a foam sheet within a water bath to simulate human skin. We then set the water to different temperatures to measure the offset. The error was not constant between different temperatures. Potential errors could involve the sensor cover, the insulation used, or the transducers used.

List of Figures

1.	Overall system design.	5
2.	Body temperature	9
3.	Zero-heat flux sensor	13
4.	Dual-heat flux model	14
5.	High-level block diagram of the proposed design.	17
6.	DHF Sensor Size and Accuracy.	18
7.	DHF Sensor Insulation Accuracy.	19
8.	Generic signal chain.	21
9.	Sensor CAD model.	22
10.	AFE schematic	24
11.	PCB CAD model.	24
12.	App	26
13.	Printed sensor	27
14.	Final sensor design	28
15.	Analog sensor on PCB	29
16.	Breadboard testing setup	31
17.	AFE on PCB	31
18.	Human test setup	33
19.	Human results	34
20.	Water bath	35
21.	Water bath test results	36
22.	Water bath test result errors	36

List of Tables

1.	Effects of CBT	10
2.	Monitoring of CBT	12
3.	Comparison of performance parameters	36

1. Introduction

Monitoring human vitals is an important action that can help people realize their conditions and how well their bodies are operating. The four main vitals include: body temperature, respiration, blood pressure, and pulse rate [1]. Each of these vitals is as important as the other. If one of these vitals begins to fail, then that could wreak havoc on the body and possibly lead to worse conditions such as death. Therefore these vitals must be closely monitored, especially for those that are susceptible to bodily fluctuations and those that are admitted into the hospital. The technology of monitoring vitals has changed drastically over the years. Each vital has its own method of monitoring such as a blood pressure cuff or something as simple as counting breaths for respiratory rate. Naturally, these technologies have evolved into more accurate, precise, and easy to use tools so that monitoring can be much more useful. Our device is used to measure CBT accurately and precisely while operating wirelessly and noninvasively. This chapter explores the motivations for measuring CBT as well as a comparison to the state of the art CBT measuring technologies.

1.1. Motivations

As the name suggests, CBT is the temperature within the core of the body. The internal organs, deep tissue, and the cerebrum. Temperature is so important because it is a prerequisite of life and without proper temperature regulation: organs can fail, metabolism rates can shift, and tissues can be damaged [2]. Although temperature on the extremities can fluctuate greatly, the core is regulated by the body's thermoregulation mechanism. Sweating and shivering are some of the body's mechanisms to regulate the core. The normal range of temperatures for the core are between 36.1 °C and 37.2 °C [3]. Two important conditions that can be a result from high or low CBT changes are hypothermia and hyperthermia. A drop to even 36 °C could bring on mild hypothermia, and 35 °C signals the person has become hypothermic [4]. An increase to 37.8-40 °C would be considered a fever, which greatly impairs bodily functions.

Figure 2 demonstrates how temperatures vary between the extremities and the core in the human body [2]. It can be noted that the core encapsulates most of the upper body (not including arms) and the head, which is also where all the internal organs are located.

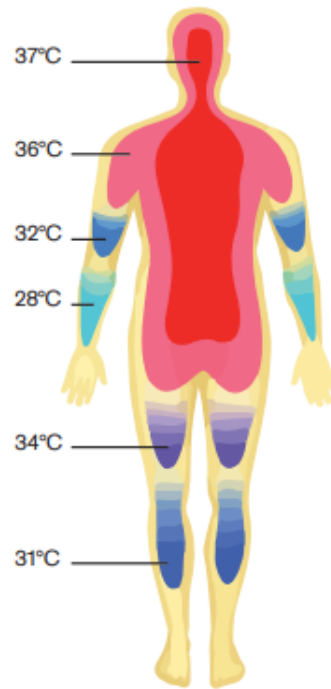


Figure 2: Diagram of how temperature is varied throughout the body [2].

1.1.1. Heat Related Illnesses

As mentioned previously, hypothermia and hyperthermia are important health conditions that relate directly to CBT. According to the Centers for Disease Control and Prevention (CDC), hypothermia is caused by prolonged exposures to cold temperatures, which result in the body not being able to produce heat as quickly as it is losing it. A lower temperature also affects the brain which can make the victim lose motor skills and affect clear thinking. Hypothermia can occur at temperatures that are not considered cold, especially if the person is chilled from sweat, rain, or submersed in water [5]. Referring to Table 1, hypothermia ranges from mild to severe as CBT drops. Severe cases lead to organ failure and death. On the other hand, hyperthermia is a state when CBT is increased beyond normal limits. Hyperthermia and fever can be more spontaneous than its hypothermia counterpart. Fever is very similar to hyperthermia but the key difference is that fever is a condition which is subject to the body's regulatory mechanism [2]. Infections and non-infectious causes can result in fever. Hyperthermia occurs when the body is unable to dissipate heat as fast as it's gaining. According to Figure ??, as CBT increases, so does the risk of

heat stroke, thermoregulatory failure and the denaturing of protein, which results in death.

Table 1: Effects of changes in CBT [2]

Temperature	Classification
$>42.6^{\circ}C$	Denaturing of protein
$40 - 42.6^{\circ}C$	Thermoregulatory failure, heat stroke
$37.8 - 40^{\circ}C$	Fever, hyperthermia
$36 - 37.8^{\circ}C$	Normothermia
$33 - 36^{\circ}C$	Mild hypothermia
$28 - 32^{\circ}C$	Hypothermia, reduced metabolism, respirator depression, loss of consciousness
$<28^{\circ}C$	Severe hypothermia, thermoregulatory failure, ventricular fibrillation, rigor, non-reactive pupils, bradycardia, cardiac arrest

1.1.2. CBT Monitoring

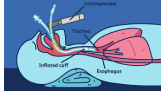
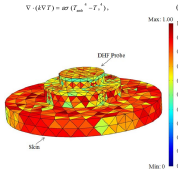
CBT holds an extremely important place in medical monitoring. Most core body temperature measurements (CBTM) are usually very intrusive to the subject. As the name suggests, to gain the most accurate reading one must measure from inside the body. Yet the need for a non-invasive way of measurement has only grown in recent years. For workers in very hot or humid environments, an accurate measure of core body temperature could serve as early detection of heat stroke, exhaustion, or hyperthermia [4]. These workers cannot have an invasive sensor and work productively. Active duty service members are another demographic that requires a consistent CBTM. Various types of heat illness and injury are a concern for the military [6]. Since the CBT of a service member in training or in the field wouldn't be measured while they are in an ideal setting, a wearable and non-invasive sensor would be desirable in order to accurately measure it.

Current measurement techniques are either relatively inaccurate and non-invasive, or accurate and invasive. The invasive techniques are more common, due to their accuracy and use in environments where the subject can be measured invasively. These include bladder inserts, intubation, or ingestion [2], [6]. Non-invasive technologies include skin thermometers [2]. However, as shown in Figure 2, core temperature can vary depending on the part of the body it is measured on. This makes most non-invasive techniques unreliable.

A comparison of current methods of CBTM is shown in Table 2. A digital fever thermometer is a basic temperature measurement device that's able to take an instantaneous temperature measurement. One would insert the tip of the device into the ear and take a measurement. Although the procedure is simple, and minimally invasive, it would be too difficult to continuously monitor temperature while holding a device inside the ear. Taking temperature measurement from the ear is nearly as accurate as a rectal measurement, which is considered the most accurate form of CBTM [7]. A forehead skin is another temperature measurement device that's able to continuously monitor the temperature of the skin on the forehead. The procedure includes placing or wrapping the device around the forehead so that it can monitor the skin temperature. This results in a noninvasive method to measure temperature, yet it isn't able to measure CBT. This device can be considered an inaccurate method for CBTM. Intubation is a CBTM that is performed during surgical procedures. Naturally, this method is extremely invasive yet yields the most accurate results since the measurement is taken from inside the core. This method is clearly only for a hospital setting and wouldn't be possible otherwise. Lastly, heat flux technology has been around for quite some time. This technology presents a way to noninvasively, continuously, and accurately monitor CBT [8]. A heat flux probe would be placed on

the forehead due to the thinness of the skin layer, and would continuously monitor CBT from there. A caveat to this technology is the use of a heater in Zero-Heat-Flux which would consume large amounts of power making it inefficient for battery operated devices. Another caveat is the long heat up time for Dual-Heat Flux which varies from 30-50 minutes until it is able to measure accurately.

Table 2: Devices to measure temperature

Method	Digital Fever Thermometer	Forehead Skin Temp Sensor	Intubation	Heat Flux
				
Invasiveness	Invasive	Noninvasive	Invasive	Noninvasive
Procedure	Insert probe into ear, rectum, etc and take measurement.	Place on forehead and continuously measure.	A surgical procedure.	Similar to forehead skin sensor except able to measure CBT.
Monitoring	Instantaneous	Continuous	Continuous	Continuous, requires heat up time.

Through the comparison, our proposed design will be focused on a device that utilizes heat flux technology. In the next chapter we'll discuss state of the art CBTM devices that have been developed from heat flux technology.

1.2. Current State of the Art

We will now discuss the current technology related to wireless wearable CBT sensors. Temperature within the core can be accurately measured using these sensors. The following will discuss different methods of noninvasive sensing and the basics of how these devices operate.

1.2.1. Zero-Heat Flux

Zero-heat flux (ZHF) is a non-invasive method that can be used in order to measure CBT. Shown in Figure 3, these thermometers consist of a thermal insulator that is

covered by a servocontrolled electric heater that eliminates heat flow through the insulator, which creates equal temperature between the insulator and the skin [9]. These thermometers can effectively measure tissue temperature approximately 1-2 cm below the skin surface, which can reasonably approximate CBT.



Figure 3: Prototype zero-heat flux sensor with two thermometers, an insulator, and a heater cover [9].

Although the ZHF is able to accurately approximate CBT, portability becomes an issue. This technology requires an external heater which can cause hindrances when attempting to make the device portable. Although the heater can be made small utilizing technology such as lithography, there is still a higher power requirement in order to run the heater. This power requirement would make it difficult to have a long lasting portable device.

1.2.2. Dual-Heat Flux

The dual-heat flux measurement is another noninvasive heat flux technology that can be used to measure CBT. This method is similar to the ZHF method with the exception of no heater and more temperature transducers. DHF operates by creating two heat channels using transducers within a thermal insulator. Assuming there is a constant and vertical heat flow, thermal equilibrium can be achieved in the thermal insulator and the subcutaneous tissue [10]. Figure 5 illustrates the implementation of a DHF sensor.

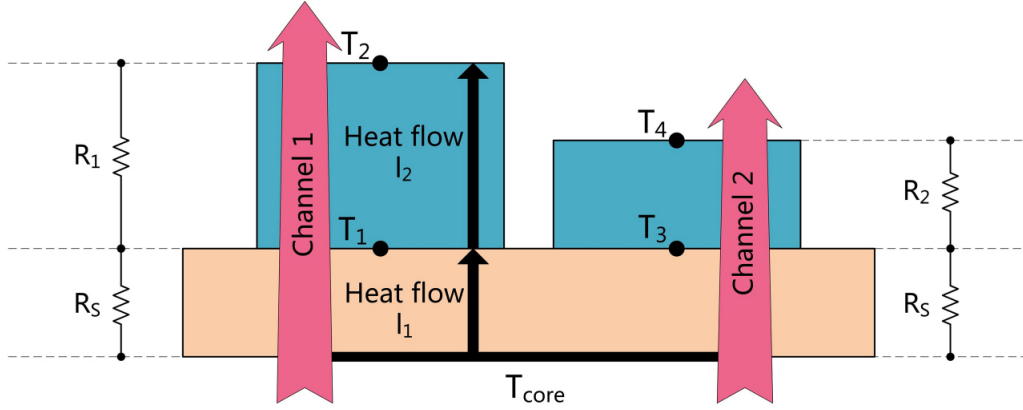


Figure 4: Dual-heat flux sensor model [11].

As illustrated in Figure 5, there are four temperature transducers placed in vertical channels which are able to sense a heat flow. This temperature difference, heat flow, and thermal resistance can be directly related to circuit theory, where we can then construct equations [10].

$$CBT = T_1 + \frac{(T_1 - T_2)(T_1 - T_3)}{K(T_3 - T_4) - (T_1 - T_2)}, \quad K = \frac{R_1}{R_2}. \quad (1)$$

Equation (1) relates temperatures at different points throughout the sensor and the ratio of resistances to the CBT. One caveat with this method is that the heat flow is assumed to travel vertically from the contact with the skin. Although this assumption is mostly accurate, some heat flow can be lost horizontally.

2. Project Overview

2.1. Design

Our proposed design allows us to wirelessly monitor CBT while maintaining low power consumption for prolonged use and wearability for the user. The design consists of a sensor, a small PCB, and a microcontroller mounted on a headband. All of the components are small and light weight that the user could wear the headband comfortably. The measurement data from the sensor is then transmitted to a mobile app that allows for real-time CBT monitoring. The design of the sensor involves a 3D printed plastic cover that acts as an insulator against ambient temperature as well as a container for our temperature transducers and main insulator. There are four analog temperature transducers placed around the cover in order to utilize DHF, which is further explained in Chapter 3. The inside of the sensor is then filled with a rubber foam insulator which also acts as a comfortable interface between the sensor and the skin of the user. The signals from the transducers are then processed through our AFE and converted to temperature measurements within the microcontroller. The measurements are then transmitted to via Bluetooth Low Energy.

The design of the AFE includes a multiplexer, an amplifier, and a two pole sallen-key filter. The multiplexer cycles through each analog temperature sensor. The selected signal is passed through to the input of the amplifier. The amplified signal goes through the filter to remove unwanted noise allowing for a pristine signal for the Analog-to-Digital Converter (ADC) of the microcontroller. The microcontroller calculates the CBT by analyzing the signals from each analog transducer. The measurement is sent to the user's phone through the Bluetooth Low-Energy (BLE) protocol.

2.2. Project Organization

This report begins with an introduction and motivation for developing a wireless CBT sensor. Chapter 3 educates the reader about the background of the DHFM and how it can be applied to wirelessly and accurately monitor CBT. Chapter 4 contains the specificities of the proposed design and how we were able to approach our final design. This chapter consolidates all the information learned from Chapter 3. Chapter 5 explains the theory and various tests that were used to implement each component in our design. Chapter 6 describes the total functionality of the design and how the interactions between each of the blocks work with each other. This chapter also discusses results of the experiment. Chapters 7 and 8 provide recommendations for future work as well as conclusions for this project.

2.3. Project Challenges

As with every new project, there are always challenges that must be faced and overcome. First and foremost, this project was conducted during COVID-19, which created challenges that many have not faced before. Such challenges include limited time for testing in the laboratory, limited interaction between peers, and limited human testing which could skew the final results. Another challenge involves the minimal real world data to compare to with our device.

3. Background Research

The background chapter will focus on the information related to the dual-heat flux technology sensors as well as constraints and necessary considerations related to each block in our proposed design. Our target end-user and constraints will ultimately guide our design choices. Figure 5 is the high-level block diagram of our proposed design.

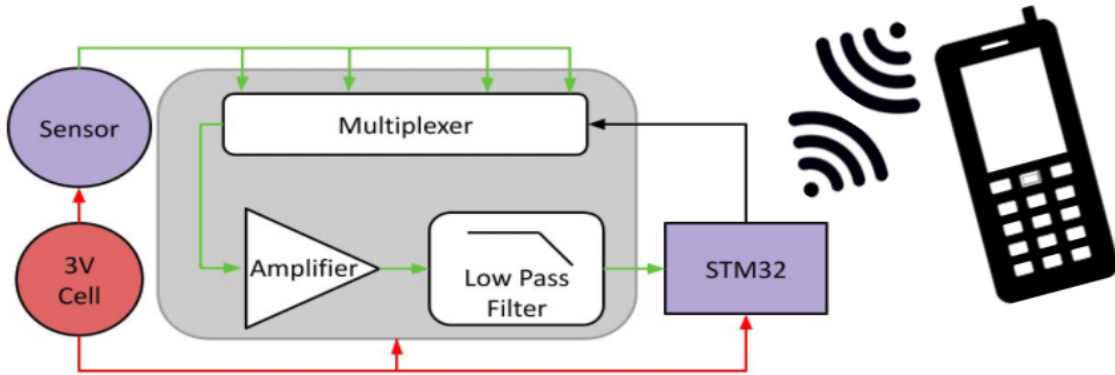


Figure 5: High-level block diagram of the proposed design.

The design begins with the sensor. This is the fundamental block of the entire device and it must be researched thoroughly in order to have good operation of the device. As temperature is converted into voltage signals through the use of transducers, the four signals are chosen by the multiplexer to pass through an amplifier and a low pass filter. After the analog stages, the information is then processed by a microcontroller and sent via BLE. The entire device will be capable of being powered by a 3 V cell battery.

3.1. Sensor Design

We have quickly discussed the operation of DHF in Chapter 1. A sensor is created with a heat transfer material surrounded by an insulating material. Inside, sensors are placed at the top and bottom of the heat transfer material. The estimated body temperature is then found using an equation Eq. (1). Although the process and building seems simple, many factors goes into the construction of the sensor. The sensor is composed of a cover, insulation, and a heat transducer. The size, type of

material used in the cover and insulation, and type of heat transducer all play a very important role in the accuracy of the sensor.

3.1.1. Sensor Size and Insulation

The size and insulation of the sensor can greatly affect the accuracy, cost, and heat up time of the device. Figure 6 shows a simulation of four different combinations of heights and describes that as the radius of the sensor increases, the error of the CBT measurement decreases.

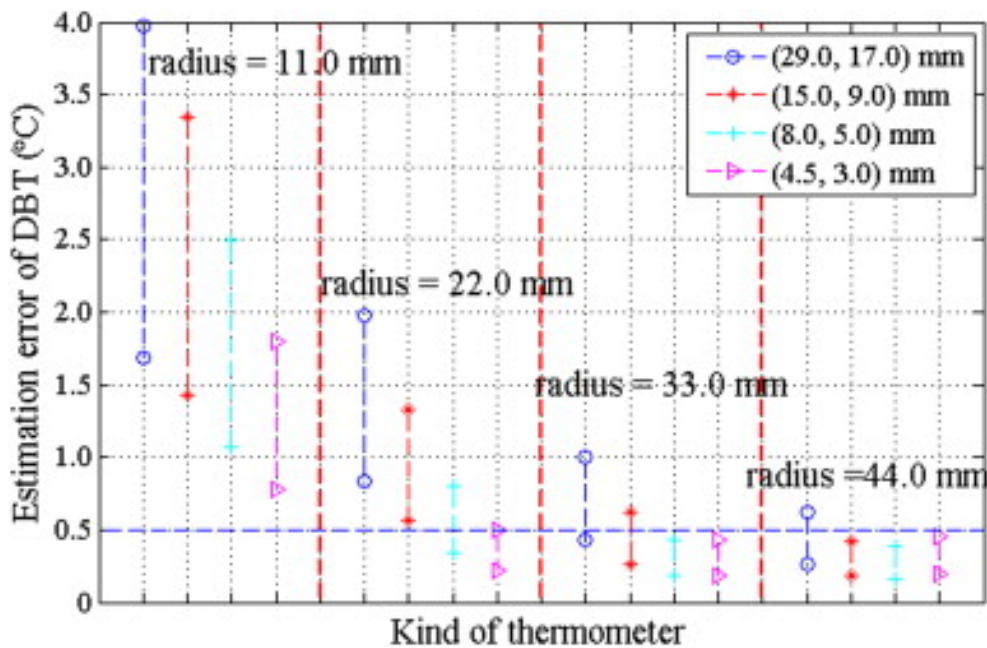


Figure 6: Size related to sensor accuracy [12].

Another important factor to take into account for the sensor size is the height. The larger the heights of the sensor are, the more error there is for the CBT estimation. It is clearly shown that as the radius increases, the heights do not affect the error as much. Therefore, when designing the size of the sensor, there should be importance on the size of the radius rather than the size of the height. Although a larger radius may result in better accuracy, comfort of the individual wearing the sensor is also important. A larger radius may be uncomfortable and may not rest well on the body.

Figure 7 shows a simulation of how the conductivity of the insulator affects the CBT estimation. The figure uses Deep Body Temperature (DBT) but this is equivalent to

CBT. The larger the conductivity of the insulator, the more error there is in CBT estimation. Therefore, when looking for an insulator, a low conductivity is preferred to have more accuracy.

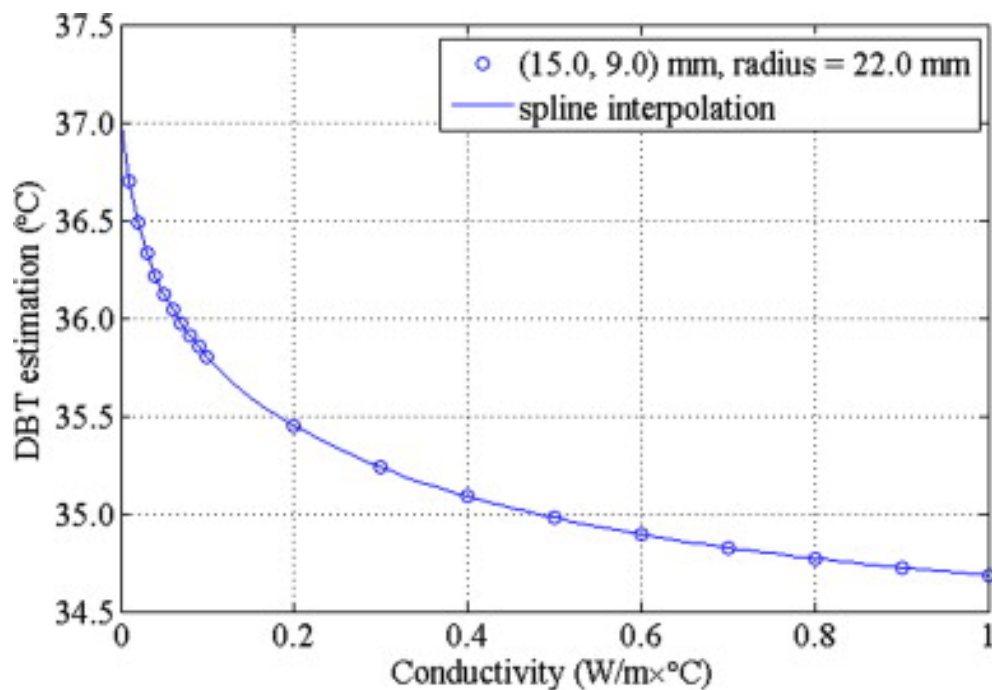


Figure 7: Insulation conductivity related to CBT accuracy [12].

3.1.2. Heat Transducers

Various types of electronic components and devices are capable of detecting and responding to changes in temperature. The most common are thermistors. Thermistors typically have an accuracy in their resistance values of $\pm 1\%$ and require an accurate current source to use effectively. Analog transducers are specially designed integrated circuits (ICs) which are usually based on temperature coefficients of diodes or other silicon devices. Typically, these devices have low power requirements and only need a stable voltage source to perform accurately. These systems usually take a voltage as an input and a voltage as an output, although a few will produce other signals out. The voltage produced will increase or decrease linearly with the temperature rising or falling. Digital transducers are similar to analog transducers, in that they are special IC packages which take a voltage in and produce a voltage out. However,

digital sensors will produce a voltage level based on a number of bits the sensor is accurate to, instead of linearly as an analog sensor will.

3.2. Electrical Design

3.2.1. Multiplexer

DHF uses the data from four transducers to calculate the CBT of an individual. An analog multiplexer was used to connect the four heat transducers to the rest of the AFE. Analog multiplexers are essentially voltage controlled switches that connect the input signals to an output pin based on a control signal. Since our signal of interest is low frequency and requires high precision the important multiplexer parameters are charge injection and switch resistance. Large amounts of charge injection and high switch resistance can affect the amplitude of the signal. Significant changes in amplitude would lead to inaccurate measurements.

3.2.2. Signal Amplification

No matter which transducers system are used, the signals coming from the sensor will have to be amplified and filtered in order to keep the integrity of the signal. First we will amplify the signal, then it will be filtered before entering the microcontroller.

For simple signal amplification, there are three topologies we can consider: A voltage follower, an inverting amplifier, and a non-inverting amplifier. The voltage follower could be used if our voltage signal was large but our current output was extremely low. For our application, we have no need for a voltage follower. An inverting amplifier would amplify and phase invert the signal. Our expected signal would be very close to DC so the non-inverting amplifier was our choice to perform the necessary amplification of our signal. The gain we choose depends on the voltage supply and the voltage output of the transducers.

3.2.3. Filtering

The next consideration is filtering out the undesired frequencies from the signal. This requires a circuit to selectively attenuate a range of frequencies for operation and pass the desired frequencies through this signal conditioning. When choosing a filter design, there can be either a passive or an active filter. The passive filter employs strictly passive components such as resistors, capacitors, and inductors. Active filters employ operational amplifiers as well as passive components in order to achieve the same goal. Passive filters can be used for simple and low power analog filtering,

but are difficult to use for very low cut-off frequencies because the values of the components would be very high. Active filtering can be used for circuits that need low frequency cut-offs as well as provide gain, but these circuits consume power and can have issues with stability. Passive filtering in this case would attenuate the signal due to the extremely high values required to achieve the low cut-off frequency.

We do not expect any signals to need a large rate of change, due to the small voltage differences between hyper and hypothermic temperatures. We also want a very low cut-off frequency to avoid high frequency noise. Therefore, the choice of an active low pass filter makes the most sense for what is expected as a signal output.

3.2.4. Microcontrollers

The microcontroller is necessary to control the system and process data. The basic signal chain is shown in Figure 8. The primary requirements for the microcontroller were low power consumption, wireless communication, and an onboard ADC. Additionally, the DHFM equations require some light data processing power. These parameters directly impact the wearability of the device. Including the ADC and wireless stack will keep the size of the final device small by eliminating additional components. Low power consumption allows for longer run time and smaller batteries. High clock speed is not important for this application due to the low data processing requirements. The most important aspect is ADC resolution, as this directly correlates to the accuracy of the final sensor.

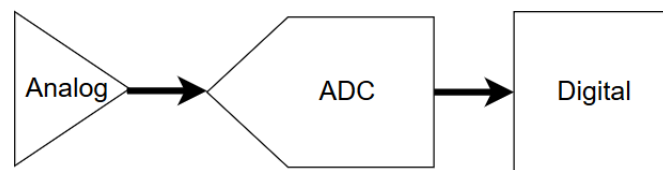


Figure 8: Generic signal chain.

4. Proposed Design and Implementation

This chapter explains the intended proposed design for our core body temperature system. This includes the various value analysis to select the components of the design.

4.1. Proposed Sensor Design

Our proposed design will enable noninvasive and wireless core body temperature monitoring. The prototype will be as small as possible to facilitate wearability. This approach will allow for CBT measurement in remote places without requiring expensive or specialized equipment. Among the primary design priorities are battery life, size, and comfort.

The first value analysis helped to determine the type of temperature sensor/-transducer. For our electrical sensing options, we chose analog transducers as our components. The value analysis chart for this choice can be viewed in Appendix A. These analog transducers should give the required amount of accuracy, as well as be in a small enough form factor to make our physical design. For the transducer, we choose the LMT70 from Texas Instruments [13]. This component combines a very small form factor with 1 percent reported accuracy and low current consumption.

The next value analysis was conducted in order to choose the type of insulation for our sensor and is shown in Appendix A. Since most of the insulation choices were very low cost, accuracy and wearability were of utmost importance. Rubber sponge foam became our choice for insulation due to it's similar resistive properties to human skin as well as its comfortability on the skin.

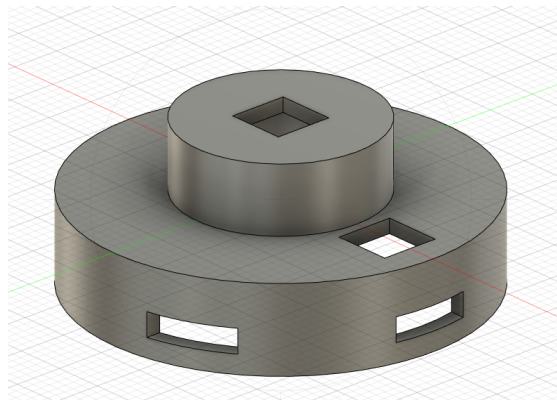


Figure 9: Sensor CAD model.

The final value analysis conducted for the sensor pertained to the sizing and can be found in Appendix A. The sizing of the sensor is extremely important in terms of accuracy and comfortability. We want to have an accurate sensor but as explained in Chapter 3.1.1, sensor accuracy became much better with larger radii. Although we would want to design a larger sensor, we have to keep comfortability in mind. In the end, we decided to go with a large radius but a small height for the sensor. Fig. 10 shows the CAD model for the sensor cover which will contain all of the components and insulation. The size was set for an outer radius of 40mm, an inner radius of 20mm, and a total height of 15mm.

4.2. Proposed Analog Front End Design

Our AFE consists of a multiplexer, an operational amplifier, and a sallen-key low pass filter. The multiplexer selects which transducer to receive signals from and pass them through the operational amplifier and filter. When looking for a multiplexer, we focused on finding one with a low turn-on resistance and that would be able to pass current through to simplify our signal chain. For breadboard testing, our through-hole choice was the MAX4617 which is an analog multiplexer with 20Ω on resistance. Unfortunately, this multiplexer did not have a surface mount device (SMD) version. Our SMD choice was the ADG804 which had a typical on resistance of 0.5Ω [14].

The operational amplifier was used for amplifying our signal while maintaining signal integrity. Our focus was on extremely low noise and low power consumption. Since we have an expected output voltage of 900mV - 1V from our analog transducers, we did not need to worry about high gain. The choice operational amplifier was the LT1636. The LT1636 boasts a $50\mu A$ quiescent current while maintaining an input offset voltage of $225\mu V$ maximum[15]. Both of these specifications are ideal in our low-power low-noise application. We propose to use this amplifier in a non-inverting configuration set for a gain of 1.5. The gain was chosen while keeping battery discharge voltage in mind so if the battery were to discharge to a lower voltage, the signal would not clip.

Lastly, the sallen-key lowpass filter was necessary to keep noise at a minimum. Since biomedical signals are very low frequency, our cut-off frequency design was set for 1 Hz. To accomplish this, we designed the sallen-key filter with the LT1636 at its core. We then used high value resistors and low value capacitors to achieve this cut-off goal. Figure 10 shows the schematic of the entire AFE.

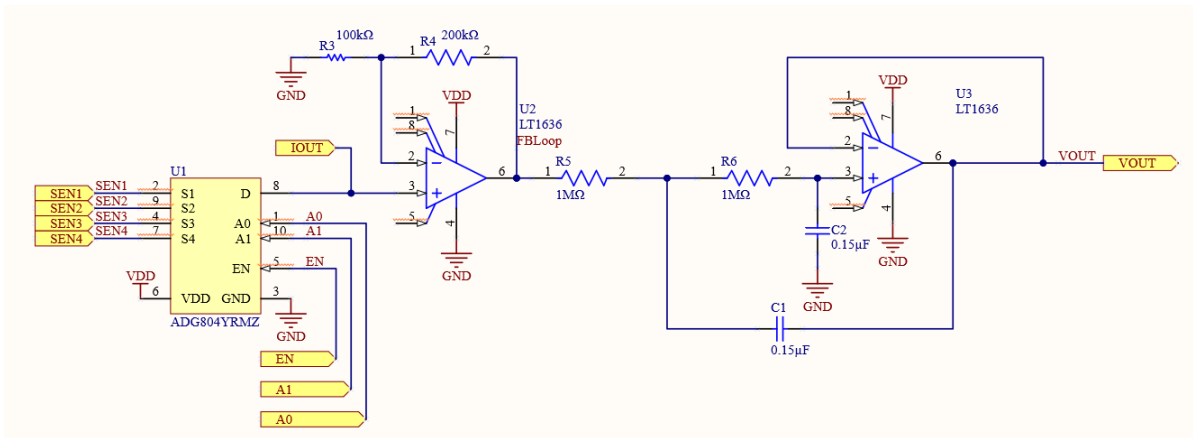


Figure 10: Analog-front end schematic design.

4.2.1. PCB Design

Once the components have been chosen and verified through breadboard testing. We began design on a printed circuit board (PCB). A PCB design was necessary for our AFE as well as each heat transducer. For the heat transducers, a simple board would be designed as small as possible. Each pin of the transducer would be traced to a small hole where a wire would connect the board to the main AFE board.

The AFE board would use a dedicated ground and power plane, as well as using internal traces, to minimize noise and distortion. Primary design considerations are maintaining signal integrity and size of the overall system. A picture of this PCB design is shown in Figure 11.

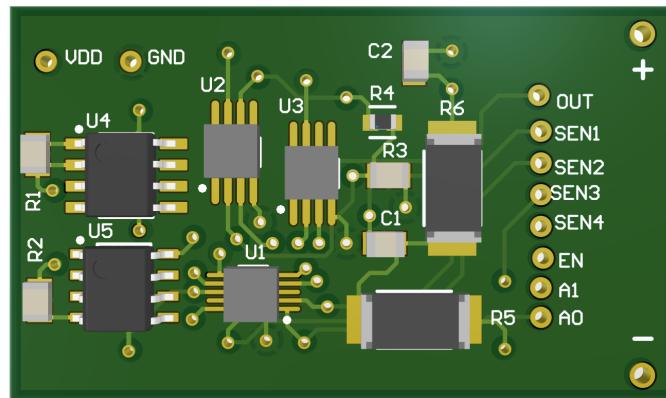


Figure 11: Analog-front end PCB design.

The final dimensions of the AFE board are 40 mm by 25 mm. This extra width allows a 3 V coin cell holder to be attached to the right side of the board, in the large plated holes. These connect to the ground and power planes to provide power to the entire circuit. Additionally, the board allows pass through to these power planes so that the microcontroller can be powered through this board as well. The final size of the transducer boards were approximately 5 mm by 5 mm.

4.3. Microcontroller, Wireless Protocol, and Mobile App

Here we explain the chosen microcontroller, wireless communication protocol, and the app used to record data. The reasoning behind our final choices is explored and the advantages and disadvantages of these components are summarized.

4.3.1. Microcontroller Options

The microcontroller options that are considered for the project are (i) ESP32 Development Board, (ii) ON Semiconductor RSL10, and (iii) STM32WB55.

We decided to use the STM32WB55 for the project based on a number of reasons[16]. The emphasis on this project was wearability, so power consumption and size were the most important factors. The STM32WB55 boasted the lowest power consumption when wirelessly transmitting and receiving data. The STM32WB55 chip also came in a Ball Grid Array (BGA) package, one of the smallest SMT mounting styles available. All of the candidates were powerful enough to perform the required signal processing and included RF front ends. As such, these parameters were less influential in the final decision process. Finally, ST provided resources for code development including example code, an initial code generator, and webinars focused on code development. The combination of these factors made the STM32WB55 the most suitable chip for our application.

The STM32WB55 will store ADC readings and transmit data over to a BLE-connected device. Excerpts from the firmware used can be found in Appendix B. The STM32WB55 offered several communication protocols including Zigbee, BLE, Wi-Fi, and BLE Mesh. We needed a short range protocol with low energy consumption that could interface with a laptop or a smartphone. BLE was the best fit for this criteria. The STM32WB55 BLE Sensor App was used to receive data from the microcontroller via BLE. This app was designed by ST specifically for STM32WB55 and other microcontrollers of that family, and allows the user to read and plot data. It also supports cloud logging for long term monitoring. A screenshot of the app is shown in Fig. 12. The following chapters provide additional details of each sub-block.

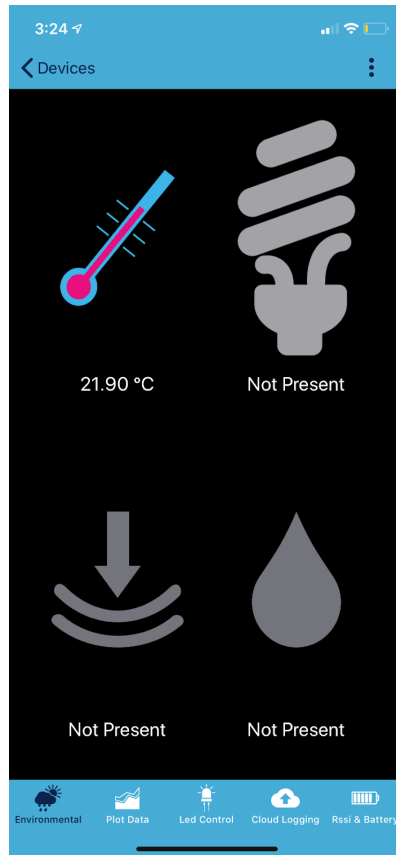


Figure 12: STM32 BLE sensor app.

5. Hardware Test Implementation

This chapter discusses tests conducted for each individual component to ensure proper functionality when combined as an entire block. This chapter supports the information that was described in Chapters 3 and 4.

5.1. Sensor

Once the sensor cover had been modeled in CAD, we printed the cover using polylactic acid (PLA) as the printing material. PLA was the choice of material due to its low cost and ease of access. PLA is also a sturdy material that can support and protect the inside of the sensor while offering some insulation from ambient temperature. Figure 13 shows the printed cover.

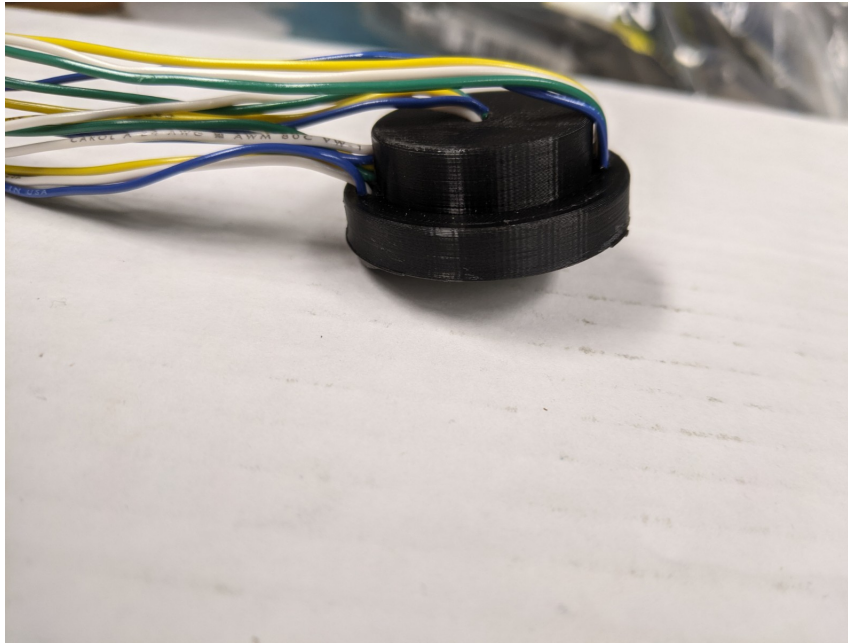


Figure 13: Printed sensor.

After the sensor had been printed, we cut and layered rubber foam within the cover. Due to the thickness of the insulation, four sheets were cut and implemented within the cover. As the insulation was being placed, the analog sensors that were in their respective PCBs were also placed in their correct positions. The positions that the sensors were in follow exactly with the dual-heat flux model described in Chapter

1.2.2. Figure 14 shows the final sensor print with the insulation and transducers properly implemented.

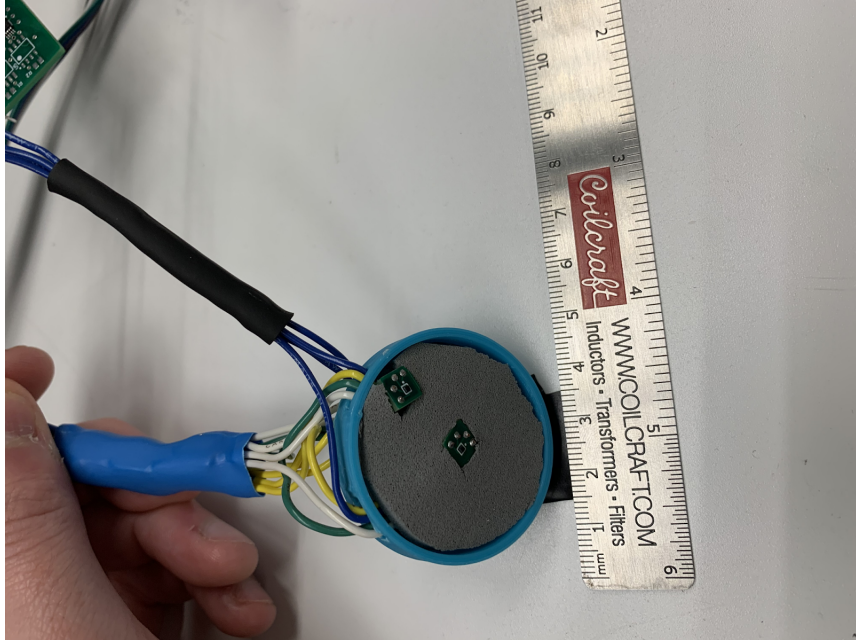


Figure 14: Final sensor.

5.2. Transducers

Here we will describe the implementation of functionality of two different transducers that were chosen for our designs. Transducers are able to convert temperature into a signal that can be read by the analog-front end.

5.2.1. Thermistor

While we waited for the analog sensor PCBs, we used thermistors in our implementation to verify use of the AFE. One side of each device was attached to the inputs of the multiplexer. The other side was connected to a common ground. A current source was connected to the output of the multiplexer. When the multiplexer would select an input by sending signals to its select pins, the current would flow through the thermistor to ground, generating a voltage signal that would be sent towards the amplifier and filter.

Initial tests of the 10 k Ω thermistor implementation were done on a breadboard with through hole components. Each thermistor started disconnected from the current source (multiplexer not activated). Each thermistor was then allowed to conduct and produce a voltage by changing the enable values on the multiplexer. The voltage was then measured with no heat applied. As a simple simulation of body heat, the active thermistor was held tightly between a technician's index finger and thumb for 30 seconds before another voltage measurement was taken.

5.2.2. Analog Sensors

The analog sensors have a much simpler implementation than the thermistor version of the sensor, as each sensor outputs a voltage signal and has power and ground pins on its package. The output pin of each sensor was tied to an input of the multiplexer, and power and ground connected to each sensor on the appropriate pins. The output voltage of the analog sensor is determined by the temperature that it senses. This relationship is governed by the following equation, where x is the voltage output of the sensor in mV:

$$^{\circ}C = (-0.193x + 212.009) \quad (2)$$

When the select pins of the multiplexer are activated, the voltage sent from the analog sensors will be directed to the input of the amplifier and filter. To test the analog sensor, we first needed to have it placed onto its PCB. Figure 15 shows the analog sensor on a PCB.



Figure 15: Analog sensor on PCB.

5.3. Operational Amplifier

As discussed previously, the op-amp is an integral component in our AFE. The amplifier was configured in a non-inverting configuration with a gain set to 1.5. The resistors used in this feedback loop were 100 k Ω and a 200 k Ω resistors. We used high values in the feedback loop so that we greatly reduced the current output by the amplifier. This in turn lowered the total power consumption of the AFE. To test the design, we powered the amplifier with 3 V and passed a small signal riding a DC offset. The expected output was an non-distorted waveform that was 1.5x the original magnitude. After confirming the operation of the amplifier, we moved to the filter block.

5.4. Active Filter

The active filter used the same operational amplifier as the our gain stage. This was set up in a Sallen Key configuration, with two poles each with a cutoff frequency of 1 Hz. This cutoff deemed acceptable as it blocks out all 60 Hz noise. The components chosen were 0.015 μF capacitors and 10 M Ω resistors. Initial testing was done using larger resistors and smaller capacitors; however, this large resistance had created a large voltage offset on the output signal, and had to be reduced. Therefore, we reduced the size of the resistors to 1 M Ω and increase the size of the capacitors to 0.15 μF . This kept the ideal cutoff frequency to 1 Hz. In order to test this filter, we passed our amplified signal into the input, which was a 1 KHz AC signal with a DC offset. We kept the frequency high to see if filter was able to block noise above 1 Hz. Once we confirmed it operated correctly at 1 KHz, we reduced the frequency until we began to see the filter passing the noise through. We were able to achieve no noise on the output until about 10 Hz.

5.5. Breadboard and Printed Circuit Board

As was previously stated, all testing initially began on a breadboard to confirm operation of our AFE. Figure 16 shows the labeled breadboard with each component block.

During this test, a current would be generated and flow into the thermistor to generate a voltage. This voltage would be selected by the multiplexer and passed through to the amplifier to be amplified. The amplified signal would then pass through the filter to be processed and ready to be digitized.

Once the design had been confirmed, we then populated the PCBs that we designed for the AFE. Figure 17 shows the AFE populated on its PCB. The PCB follows the

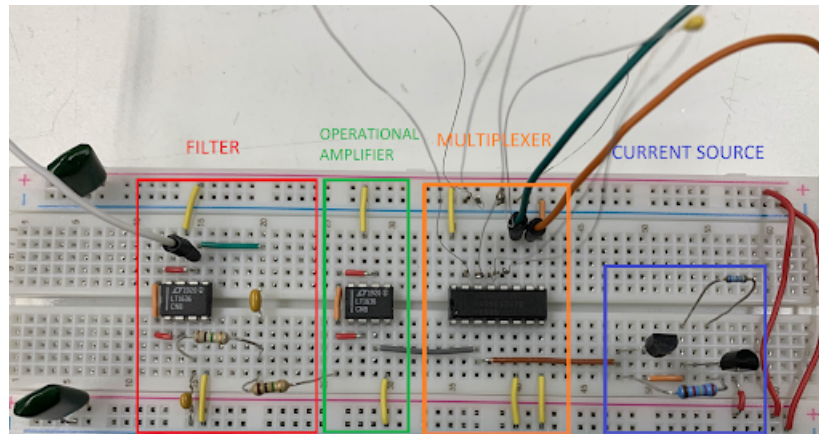


Figure 16: Breadboard testing setup.

same configuration as the breadboard with the exception of thermistors and current source. For the PCB, we used the analog sensors. In order to test the PCB, we followed a similar approach to the breadboard and introduced a small signal riding a DC offset to measure the output. Once the operation of the PCB had been confirmed, we then used the microcontroller to select the multiplexer pins of U1. We also soldered the outputs lines from the analog sensors and powered the board.

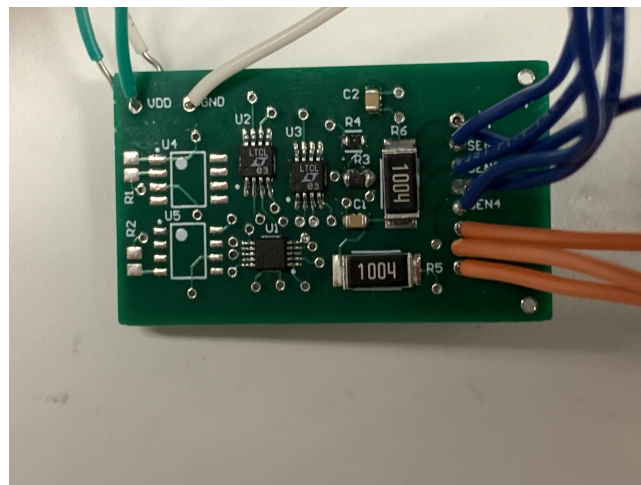


Figure 17: AFE on PCB.

5.6. Microcontroller

The microcontroller is used to process the data from the AFE and send it wirelessly to the user's smartphone via BLE. It is connected to the multiplexer to control the selected transducer.

5.6.1. Code and Implementation

The microcontroller firmware was developed with the help of an STM workshop [17]. It initializes the required peripherals and enters a basic loop until the sensor is powered off. When the sensor is powered on, the microcontroller initializes the ADC and the RF front end. It then waits for a smartphone to connect. Once a connection is established the microcontroller enters a loop. First, the data from each temperature sensor is digitized with the ADC and stored in a variable. The multiplexer is switched between ADC readings so all sensors are sampled. Once the data from each sensor is stored the user's CBT is calculated using Equation 2. The estimated temperature reading is formatted into 8 bits and appended to a timestamp. This packet is then sent to the connected smartphone via a BLE notification. The loop repeats approximately every second until the device is powered down or the smartphone is disconnected. In the event of a disconnect, the sensor will return to the waiting state until a BLE device is connected again.

The code had multiple parts that needed to be tested. The first section we verified was the multiplexer switching routine. This was tested by connecting the corresponding I/O pins to an oscilloscope and verifying that the correct binary sequence was sent in an appropriate time window. The next functionality tested was the ADC functionality. A test signal from a bench power supply was fed into the ADC. An LED was illuminated on the board if the measured voltage was below a threshold and turned off if it rose above the threshold. This was repeated with different thresholds to verify the ADC was accurate across the 0 to 3 volt range. The final section tested was the BLE communication. In order to test this a dummy value was sent to the connected smartphone. This value was incremented every time data was sent to verify all the packets arrived.

Once every subsection of the microcontroller code was tested we verified the functionality of the entire system. A set voltage was applied to the multiplexer pins to emulate the output of the temperature transducers. These voltages were digitized by the ADC and converted to a single CBT measurement. This data was then sent to a smartphone using BLE.

6. System Integration and Data Analysis

This chapter discusses the implementation and testing of the sensor on humans and a heated water bath. Both of these were used to see how the sensor behaves while on a human as well as how the sensor behaves while temperature is varied between a specific range.

6.1. Human Test Implementation

Initial tests were done by attaching the sensor to the subjects forehead via pressure from a headband. A picture of the setup is shown in Figure 18. The subject was to be in resting position and not move while testing, in order to ensure good sensor contact. The sensor was placed on the subjects temple. During this test, the system as powered by a 3 V power supply rather than a 3 V coin cell. Before testing began, the subjects temperature was recorded with an oral thermometer was a baseline reading.



Figure 18: Human test setup.

Figure 19 shows the results of a human trial. The graph shows that the sensor's heat up time is very fast, about seven minutes compared to a 23.5 minute heat up time by [11]. However, the sensor did not reach the expected temperature of 37 °C. The highest temperature measured by the sensor was approximately 35 °C. A 2 °C offset is too large to ignore, especially when considering the change in the core body temperature range. The next round of tests were performed to determine if the offset was consistent at different temperatures.

Test on Human Subject

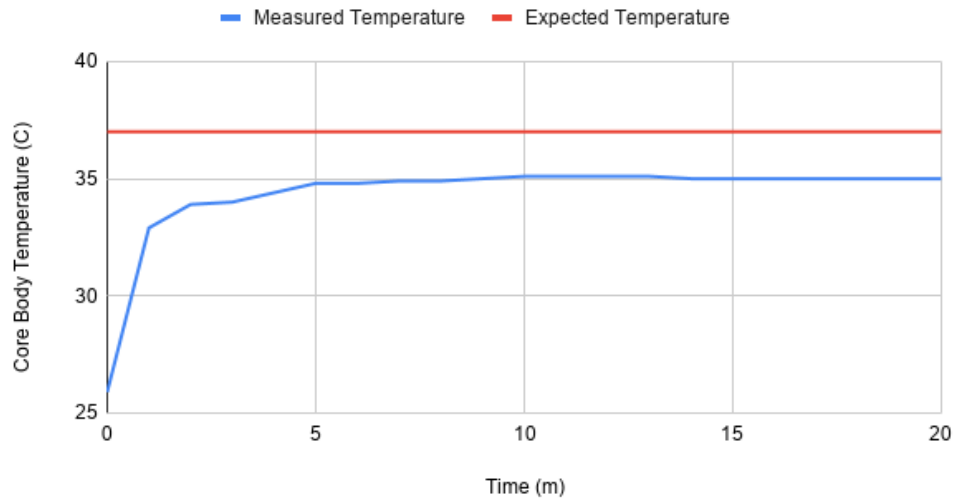


Figure 19: Result of a human trial (measured temperature in blue, expected temperature in red).

6.2. Water Bath Testing

After initial human tests, a water bath test was devised to investigate levels of offset and error in the system. The sensor was affixed to a rubber sheet that was placed on top of the water bath. A picture of the water bath is shown in Figure 20. This acted as a model for human tissue where the rubber simulates skin and the water temperature acted as the core temperature. The test was performed at different temperatures ranging from 32 °C to 40 °C and the difference between the water temperature and the measured temperature was recorded. These offsets are shown in Figure 21.



Figure 20: The water bath used for testing.

The offset varied from 4.9 °C up to 10 °C with a water temperature of 32 °C and 40 °C, respectively. This variation makes it very difficult to compensate the offset in the microcontroller firmware.

Since the offset wasn't consistent amongst different temperatures, we considered possible solutions for the issue at hand. i) First, the sensor cover had many holes in it for wire access. These holes could have potentially caused insulation issues. ii) Ambient temperature could have been affecting the isolation of the sensors much more than we expected. iii) Another issue we considered is the insulation implementation. We cut four sheets of foam insulation and inserted them into the sensor cover. The insulation most likely had air pockets within the cover which could have caused non-uniform heat flow within the insulation. iv) Lastly, we considered changing the analog sensors that we used. The analog sensors are specified at a much larger temperature range with a large variation in voltage on small changes of temperature. We would have liked to use a transducer with a smaller range and less sensitivity to temperature. Further discussion of recommendations are proposed in Chapter 7.

Table 3 shows a short comparison our our work to other works. Our initial response time is much quicker than other works similar to ours but our accuracy is not up to par with the other works.

Table 3: Comparison of performance parameters

Parameters	[11] Feng et al	[18] Huang et al	This Work
Sensor Accuracy	$<\pm 0.1^{\circ}\text{C}$ @ 30 – 40°C	$0.009 \pm 0.037^{\circ}\text{C}$ @ 22 – 42°C	-2°C @ 37°C
Initial Response	20 min	23.5 min	7 min

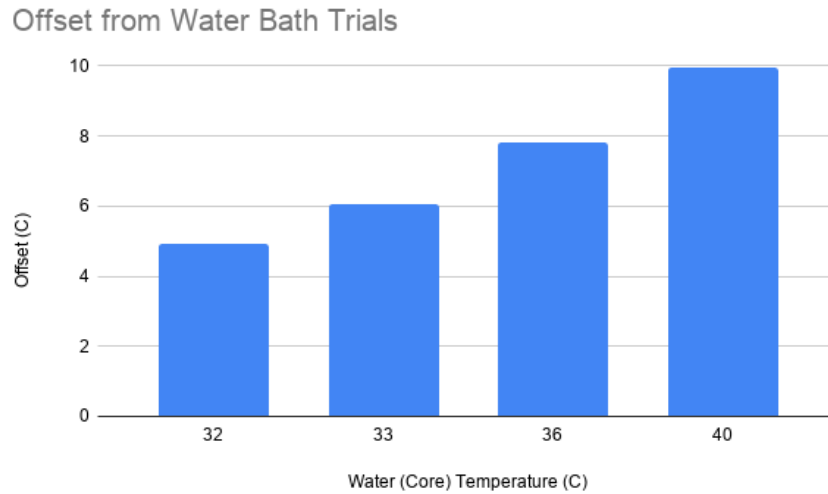


Figure 21: Temperature offset from water bath trials done at 32, 33, 36, and 40 °C.

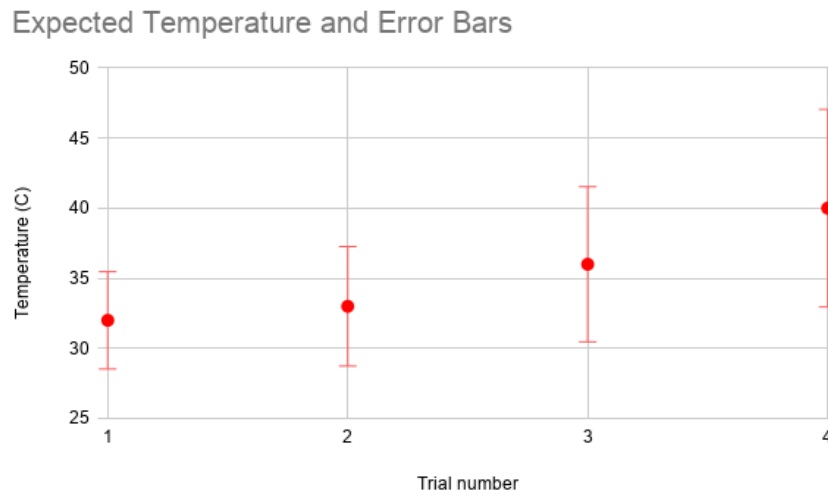


Figure 22: Dots represent expected temperature, error bars are based on the measured temperature.

7. Recommendations

In this chapter, we detail the various improvements to the core body temperature measuring device. Results from our tests did indeed prove the concept of a CBT measuring sensor, but left much to be desired. These improvements will be elaborated on in two areas; transducer choice and sensor fabrication. Fabrication will include materials, design, and build techniques.

7.1. Transducer Considerations

When choosing transducers for our sensor implementation, our main considerations were power consumption, size, and accuracy. In terms of power consumption, these design considerations have not changed from the initial proposal. Transducers with lower power draw are preferable to those with higher draw. However, size and accuracy came with unforeseen problems.

7.1.1. Sensor Accuracy vs Rate of Change

The LTM70 is a remarkable sensor, with the ability to have extremely good accuracy within ranges of temperatures about 20-30 °C of each other. However, the wide operating range meant that the rate of change per degree was very small. In an application which needs to measure in a wide range, this is an excellent attribute. With our implementation, this became a disadvantage. Our expected temperature range is about 5 degrees wide. With the sensors expected rate of change of about 6 mV per degree, this means our entire temperature range has a change of about 24 mV. Given that everything runs on a 3 V source, our gain is capped at very small values. This makes it extremely difficult to extract a meaningful difference between measurements. With our gain of 1.5, the rate of change becomes 9 mV per degree. Even an offset of 1 mV in our amplifier, filter, or ADC can thus have drastic impacts on the measurements calculated by our microcontroller.

7.1.2. Sensor Size

Initially, it was thought that smaller sensors would be ideal. They would allow an easier build and a smaller overall design. However skin contact became an issue early on in prototype testing. The LT770 was so small that it meant the solder joints connecting the wires to the sensor board would sometimes interfere with good skin contact. They did make the mechanical build process go easier, but the soldering process was more advanced in difficulty, with sensors being so light that hot air rework

station would often blow them away, even on low settings. Additionally, although the sensor size was small, it needed 4 external connections. This gave a total of 16 wires which had to be passed thru the physical shell. This meant larger cutouts and more space for external temperatures to invade the shell.

7.2. Physical Design Considerations

The physical design effort for this device was somewhat hampered by laboratory restrictions and manufacturing abilities. There were several improvements that could be made with both the material of the cover and insulation.

7.2.1. Cover Material and Design

The cover for the CBT sensor need the characteristics of being a good shield from external temperature as well as being light enough to not fatigue the wearer. Polylactide (PLA) plastic fits these characteristics, however the method of additive manufacturing via 3-D printer introduces challenges. These included small holes from the extrusion of material, as well as rough surfaces on the inside of the sensor, where the insulation was to be placed. This created both gaps in insulation from poor density and allowed more outside air to affect the flow of heat inside the sensor. Injection molding or some other manufacturing process would create smoother lines and ensure no extra gaps. Additionally, smaller cutouts for wires could increase the shell's effectiveness. These cutouts are large for the wires that are being fed thru, and could be allowing lows of outside air to interfere with the heat flow inside the system.

7.2.2. Insulating Material

The insulating material inside the sensor shell should have the ability to transmit heat along the dual channels but also have enough thermal mass slow the rate at which this heat flows. Our rubber sheet was a good material from that aspect, but we had issues packing the sheet dense enough into the sensor to completely insulate it. Each piece of foam had to be hand cut to fit the sensor, and these cuts had some level of inaccuracy. This caused further gaps inside the system which could introduce error.

7.3. Microcontroller and Mobile App

The microcontroller firmware and the mobile app provide basic functionality but lack important power saving and user friendly features. These issues can be addressed by

improvements outlined in the following sentences.

7.3.1. Data Acquisition

The current code only takes one sample from each sensor per CBT calculation. This means that glitches and noise on the input signals will have a large impact on the calculated temperature. Implementing a rolling average would lessen the impact of noise and increase the reliability of the system.

7.3.2. Power Reduction

The microcontroller is currently the biggest power draw in the system. There are a couple changes that could be implemented to significantly improve efficiency. Increasing the time between BLE notifications would lower power used for the RF front end. The RF front end draws a significant amount of power to send and receive data wirelessly. It is configured to send data every second. This interval is overkill for our application and contributes to the excessive power consumption. As the measured temperature does not change very fast, even during the heat up time, making this interval longer would conserve power and maintain accuracy. Another method to reduce power consumption is putting the microcontroller into a low power mode when it is not processing or sending data. This would turn off peripherals and clocks when they are not in use.

7.3.3. User Interface

Data was collected using the STM BLE Sensor application. While functional, the app lacks features like data logging and plotting over long time frames. A custom application that automatically exported data to a file would simplify data collection and make longer trials more feasible.

8. Conclusion

The measurement of Core Body temperature is important value in many situations. Detecting a dropping or rising temperature could allow early detection of a dangerous condition in multiple environments. Using the principles of the dual-heat flux method, a design can be fabricated using four temperature sensors in a single shell. An analog filtering and amplification stage would take in signals from these transducers and send them to a microcontroller for processing. During initial design stages, analog transducers were chosen, as well as the STM family of microcontrollers. Testing was conducted on both human subjects and in a controlled synthetic environment involving a water bath and rubber as a skin substitute. In both tests, a significant offset was seen between the temperature measured by an oral thermometer and the output of the system. The system is a viable first attempt and various adjustments can be made to improve the performance and accuracy.

Acknowledgment

We would like to thank our MQP advisor Professor Ulkuhan Guler for her guidance and patience. Furthermore, we would like to thank William Appleyard in the ECE shop for assisting us with our parts and material orders, and Professor Billiar for helping us acquire the water bath used for testing. We would also like to express our gratitude towards Ian Costanzo and Devdip Sen, and the ICAS lab for their constructive feedback throughout this project. Finally, we would like to thank our friends and family for their continuous support and patience.

References

- [1] F. M. McCarthy, "Vital signs at the six-minute warnings," *The Journal of the American Dental Association*, vol. 100, no. 5, pp. 682–691, 1980.
- [2] D. M. GmbH, "The significance of core temperature - pathophysiology and measurement tools," 2015. [Online]. Available: <https://www.draeger.com/Products/Content/tcore-bk-9068132-en.pdf>
- [3] H. Yousef and M. Varacallo, "Physiology, thermal regulation," *StatPearls*, 2018.
- [4] K. J. Dunleavy, "Which core body temperature measurement method is most accurate?" *Nursing2020*, vol. 40, no. 12, pp. 18–19, 2010.
- [5] C. for Disease Control and Prevention, "Hypothermia|winter weather," 2019. [Online]. Available: <https://www.cdc.gov/disasters/winter/staysafe/hypothermia.html>.
- [6] A. M. Andrews, C. Deehl, R. L. Rogers, and A. L. Pruziner, "Core temperature in service members with and without traumatic amputations during a prolonged endurance event," *Military medicine*, vol. 181, no. suppl_4, pp. 61–65, 2016.
- [7] M. Medicine, "Fever temperatures: Accuracy and comparison," 2019.
- [8] A. Bräuer, A. Fazliu, T. Perl, D. Heise, K. Meissner, and I. F. Brandes, "Accuracy of zero-heat-flux thermometry and bladder temperature measurement in critically ill patients," *Scientific Reports*, vol. 10, no. 1, pp. 1–7, 2020.
- [9] Y. Eshraghi, V. Nasr, I. Parra-Sanchez, A. Van Duren, M. Botham, T. Santoscoy, and D. I. Sessler, "An evaluation of a zero-heat-flux cutaneous thermometer in cardiac surgical patients," *Anesthesia & Analgesia*, vol. 119, no. 3, pp. 543–549, 2014.
- [10] K.-I. Kitamura, X. Zhu, W. Chen, and T. Nemoto, "Development of a new method for the noninvasive measurement of deep body temperature without a heater," *Medical engineering & physics*, vol. 32, no. 1, pp. 1–6, 2010.
- [11] J. Feng, C. Zhou, C. He, Y. Li, and X. Ye, "Development of an improved wearable device for core body temperature monitoring based on the dual heat flux principle," *Physiological measurement*, vol. 38, no. 4, p. 652, 2017.

- [12] M. Huang, T. Tamura, W. Chen, and S. Kanaya, "Evaluation of structural and thermophysical effects on the measurement accuracy of deep body thermometers based on dual-heat-flux method," *Journal of thermal biology*, vol. 47, pp. 26–31, 2015.
- [13] "Precision Analog Temperature Sensor, RTD and Precision NTC Thermistor IC," Texas Instruments, 2015. [Online]. Available: <https://www.ti.com/lit/ds/symlink/lmt70.pdf>
- [14] "0.5 Ω CMOS 1.65 V to 3.6 V 4-Channel Multiplexer," Analog Devices, 2020, rev.B. [Online]. Available: <https://www.analog.com/media/en/technical-documentation/data-sheets/ADG804.pdf>
- [15] "Over-the-top micropower rail-to-rail input and output op amp," Analog Devices, 1998, rev.D. [Online]. Available: <https://www.analog.com/media/en/technical-documentation/data-sheets/1636fc.pdf>
- [16] "Bluetooth[®] Low Energy and 802.15.4 Nucleo pack based on STM32WB Series microcontrollers," STMicroelectronics, 2019, rev.2. [Online]. Available: https://www.st.com/resource/en/user_manual/dm00517423-bluetooth-low-energy-and-802154-nucleo-pack-based-on-stm32wb-series-microcontrollers-stmicroelectronics.pdf
- [17] "Stm32wb workshop," STMicroelectronics, 2019. [Online]. Available: https://www.st.com/content/st_com/en/support/learning/stm32-education/stm32-moocs/STM32WB_workshop_MOOC.html
- [18] M. Huang, T. Tamura, Z. Tang, W. Chen, and S. Kanaya, "A wearable thermometry for core body temperature measurement and its experimental verification," *IEEE journal of biomedical and health informatics*, vol. 21, no. 3, pp. 708–714, 2016.

A. Decision Matrices

Table A.1: Value Analysis for Transducer Type

Transducer	Analog Transducer	Digital Transducer	Thermistors	Lithography
Accuracy	3	3	4	3
Heat up Time	5	5	5	5
Cost	4	4	4	1
Complexity	5	3	3	1
Wearability	5	5	5	5
TOTAL	63	61	66	53

Table A.2: Value Analysis For Sensor Size

Size	Large Radius Large Height	Large Radius Small Height	Small Radius Large Height	Small Radius Small Height
Accuracy	4	5	2	3
Heat up Time	1	3	2	4
Cost	3	4	4	5
Complexity	5	5	5	5
Wearability	1	4	3	5
TOTAL	36	59	41	62

Table A.3: Value Analysis for Insulating Material

Insulator	Rubber Sponge	Nylon	Polystyrene	Cork
Accuracy	3	1	5	4
Heat up Time	4	5	2	3
Cost	5	5	5	5
Complexity	5	5	5	5
Wearability	5	3	4	3
TOTAL	62	47	62	56

B. Microcontroller Firmware

B.1. Data Acquisition using ADC

```
uint16_t ADCRead(void)
{
    if (HAL_ADC_Start_IT(&AdcHandle) != HAL_OK)
    {
        /* ADC conversion start error */
        Error_Handler();
    }

    /* Wait till conversion is done */
    while (ubAdcGrpRegularUnitaryConvStatus == 0);

    return uhADCxConvertedData_Voltage_mVolt;
}
```

B.2. Convert Data from mV to °C

```
uint16_t mvtot(uint16_t mv)
{
    mv -= 11; //remove measured offset
    mv = mv/1.5; //scale based on amplifier gain
    temperature = (-0.193*mv + 212.009)*10; //convert to temperature
    return temperature;
}
```

B.3. Transmit Data to Smartphone via BLE

```
static void TEMPLATE_Send_Notification_Task(void)
{
    uint8_t value[4];
    uint8_t i;
    uint16_t raw_values[4];
    uint16_t temp_values[4];
}
```

```

uint16_t temp;
temp = 0;
i = 0;
for(i = 0; i<4; i++) //switching for MUX pins
{
    switch (i)
    {
        case 0:
            break;

        case 1:
            HAL_GPIO_TogglePin(GPIOB, GPIO_PIN_6);
            HAL_Delay(50);
            break;

        case 2:
            HAL_GPIO_TogglePin(GPIOA, GPIO_PIN_8);
            HAL_GPIO_TogglePin(GPIOB, GPIO_PIN_6);
            HAL_Delay(50);
            break;

        case 3:
            HAL_GPIO_TogglePin(GPIOB, GPIO_PIN_6);
            HAL_Delay(50);
            break;

        default:
            break;
    }
    raw_values[i] = ADCRead();
    temp_values[i] = mvtot(raw_values[i]);
}

temp = temp_values[0] + (((temp_values[0] -
    temp_values[1])*(temp_values[0] -
    temp_values[2])))/(2.4*(temp_values[2] - temp_values[3]) -
    (temp_values[0] - temp_values[1]));

HAL_GPIO_TogglePin(GPIOB, GPIO_PIN_6);
HAL_GPIO_TogglePin(GPIOA, GPIO_PIN_8);

```

```

value[0] = (uint8_t)(TEMPLATE_Server_App_Context.Temperature.TimeStamp &
    0x00FF);
value[1] = (uint8_t)(TEMPLATE_Server_App_Context.Temperature.TimeStamp
    >> 8);
value[2] = (uint8_t)(temp & 0xFF);
value[3] = (uint8_t)(temp >> 8);

TEMPLATE_Server_App_Context.Temperature.Value +=
    TEMPLATE_Server_App_Context.ChangeStep;
TEMPLATE_Server_App_Context.Temperature.TimeStamp +=
    TEMPERATURE_CHANGE_STEP;
if (TEMPLATE_Server_App_Context.Temperature.Value >
    TEMPERATURE_VALUE_MAX_THRESHOLD) {
    TEMPLATE_Server_App_Context.ChangeStep = -TEMPERATURE_CHANGE_STEP;
}
else if (TEMPLATE_Server_App_Context.Temperature.Value <
    TEMPERATURE_VALUE_MIN_THRESHOLD)
{
    TEMPLATE_Server_App_Context.ChangeStep = +TEMPERATURE_CHANGE_STEP;
}

if(TEMPLATE_Server_App_Context.NotificationStatus)
{
    #if(CFG_DEBUG_APP_TRACE != 0)
        APP_DBG_MSG("-- TEMPLATE APPLICATION SERVER : NOTIFY CLIENT WITH
            NEW PARAMETER VALUE \n ");
        APP_DBG_MSG(" \n\r");
    #endif
    TEMPLATE_STM_App_Update_Char(0x0000,(uint8_t *)&value);
}
else
{
    #if(CFG_DEBUG_APP_TRACE != 0)
        APP_DBG_MSG("-- TEMPLATE APPLICATION SERVER : CAN'T INFORM CLIENT -
            NOTIFICATION DISABLED\n ");
    #endif
}
return;
}

```
